J Mol Model (2013) 19:2265–2271
DOI 10.1007/s00894-012-1739-y

ORIGINAL PAPER

Molecular dynamics study of hell's gate globin I (HGbI) from a methanotrophic extremophile: oxygen migration through a large cavity

E. Irene Newhouse · James S. Newhouse · Maqsudul Alam

Received: 23 September 2012 / Accepted: 14 December 2012 / Published online: 2 February 2013

Abstract Hell's gate globin I (HGbI), a heme-containing protein from the extremophile *Methylacidiphilum infernorum,* has fast oxygen-binding/slow release characteristics due to its distal residues Gln and Tyr. The combination of Gln/Tyr distal iron coordination, adaptation to extreme environmental conditions, and lack of a D helix suggests that ligand migration in HGbI differs from other previously studied globins. Locally enhanced molecular dynamics trajectories of oxygen migration indicate a large internal cavity. This may increase the tendency of oxygen to exit from portals other than the most direct exit from the space near the heme. Oxygen may reside transiently in shallow surface depressions around the exits. Such surface trapping may enhance both oxygen uptake by increasing contact time between molecules, and decrease release by increasing the probability of oxygen reentry from the vicinity of the portal.

Keywords Globin · Extremophile · Locally enhanced sampling · Molecular dynamics · Oxygen migration

Introduction

Globins are heme-containing oxygen-binding proteins best known for their oxygen transport activity. However, they also perform diverse functions such as NO scavenging, nitrate reductase, nitrate dioxygenase, and peroxidase activities, oxygen sensing, sulfide transport, as well as gene regulation [1]. The crystal structure of hell's gate globin I (HGbI), from *Methylacidiphilum infernorum*, an acidophilic (optimal growth pH is 2.0), thermophilic (optimal growth temperature is 60C) methanotroph [2], has recently been determined [3]. There is a glutamine at E7, the position occupied by the distal histidine in many other globins, as well as a tyrosine at B10. As do other globins with these distal residues [4, 5], HGbI binds oxygen rapidly, and has an unusually slow off-rate [3]. The physiological role of HGbI has yet to be determined. Its oxygen kinetics does not suit it for oxygen transport. HGbI lacks a D helix, which compresses the region occupied by the distal pocket in other globins. The combination of Gln/Tyr distal iron coordination, adaptation to extreme environmental conditions, and lack of a D helix suggests that ligand migration in HGbI differs from other previously studied globins.

In locally enhanced sampling (LES) molecular dynamics (MD), multiple copies of the ligand diffuse through the protein. The protein-ligand interactions are scaled to shorten the time-scale of the simulation [6] and increase the ligand exit rate. LES simulations have been used to study ligand migration in myoglobin [6, 7], lupine leghemoglobin [8], human cytoglobin [9], a hemoglobin from the worm *Cerebratulus lacteus* with no A helix [10], a fruitfly hemoglobin [11], truncated hemoglobin O of *Mycobacterium tuberculosis* [12], and tetrameric human hemoglobin [13]. Leghemoglobin is the only one of these systems to show ligand exit only via the direct pathway. In the other systems, exits occur from several locations, which do not appear to be conserved. While one might expect exits from helix turns, where the less-ordered residues might be more flexible, exits also occur between helices.

CO diffusion paths in myoglobin (SPMb) have also been studied via direct molecular dynamics computations.

E. I. Newhouse (✉) · J. S. Newhouse
129 Walua Place,
Kihei, HI 96753, USA
e-mail: einew@hotmail.com

M. Alam (✉)
Department of Microbiology, University of Hawaii,
2538 McCarthy Mall, Snyder 111,
Honolulu, HI 96822, USA
e-mail: alam@hawaii.edu

Several studies have focused on the movement of CO between transient internal docking sites after photodissociation [14–16]. Molecular dynamics calculations have also been used to elucidate the infrared spectra of CO within SPMb [17]. Ligand migration seems to involve correlated protein conformational changes [15, 18, 19]. These works compare their results to time-resolved x-ray crystal structural studies. Ruscio et al. performed multiple long simulations to study exit from and entrance into SPMb [20]. CO diffuses from the distal pocket into the rest of the protein via two transiently open gates in the protein interior. The two most favorable exit portals are near the heme. There has been experimental evidence to support the existence of alternate diffusion pathways in SPMb from comparison with mutagenesis studies [21] and picosecond-resolution x-ray crystal structures [22, 23]. Work on CO diffusion in myoglobin was reviewed by Elber [24] in 2010.

CO diffusion pathways in SPMb have also been mapped by potential of mean force calculations from molecular dynamics trajectories computed with temperature-accelerated MD [25]. Potential of mean force calculations from direct MD by implicit ligand sampling have also been done on SPMb [26]. The method has also been applied to other globins [27] and references therein.

Anselmi et al. [28] studied neuroglobin (the globin of known structure most homologous to HGbI [3]) (Ngb) by molecular dynamics simulations. Most of the exits in murine Ngb were between the G helix and AB turn; Anselmi et al. saw no exits from the direct pathway. Bocahut et al. [29] used metadynamics and coarse-grained MD to study ligand dynamics in human Ngb as a function of oxidation states and ligand. Only some of the exits were common to more than one of the cases examined. Bocahut et al. also saw little exit via the direct pathway in Ngb. In spite of the fact that crystalline Ngb only binds Xe in two of the four Xe pockets observed in SPMb, these computational studies indicate that positions homologous to all four SPMb Xe sites are transient binding pockets for gaseous ligands. Lutz et al. [30] studied CO migration in Ngb using Fourier transform-temperature-derivative spectroscopy and molecular dynamics calculations, finding seven transient docking sites in addition to the distal pocket.

We undertook an LES study of hell's gate globin I (HGbI), to compare its O_2 migration properties with those globins previously studied and identify characteristics which might contribute to its oxygen-binding properties.

Methods

Locally enhanced sampling molecular dynamics calculations using NAMD [31] were set up along similar lines to Orlowski and Nowak [9], including use of CMO oxygen type for O_2. However, we ran 5 ns trajectories, rather than 2.5 ns, and with 5 or 10 copies of O_2. 50 trajectories were computed. Periodic boundary conditions, 1–4 scaling with scale factor 1.0 and dielectric 1.0 were used. The switch distance was 8 Å, the cutoff 12 Å, and the pair list distribution 13.5 Å. The margin was 1.0 Å, 20 steps/cycle, rigid bonds, tolerance 0.0001, and iterations 100. PME electrostatics was used. The structure was first minimized for 50,000 cycles with the protein, heme, and oxygen fixed. The minimized structure was heated to 310 K over 500,000 steps reassigning every step with an increment of 0.001. Once again, the oxygen was fixed. In a subsequent step, the system was equilibrated at 310 K, still with fixed oxygen, using Langevin temperature control (damping coefficient 5, hydrogens not coupled to bath) and the NPT ensemble with Langevin pressure control (P=1 atm, piston period 100, piston decay 50, piston temp 310) for 0.2 ns. For the MD, the oxygen was allowed to move under the same conditions.

Trajectories were analyzed with VMD [32]. Internal volumes were computed using the Castp server [33], with the default probe radius of 1.4 Å, and plotted with Chimera [34]. Hydrogen-bond analyses were done with the H-bonds plugin in VMD, with the distance between heavy atoms set to 3.5 Å and the donor-H-acceptor angle limited from 120 to 180 deg. Ligand volume occupancies were computed using the Volmap tool in VMD.

Results

Internal cavities in crystalline sperm whale myoglobin (SPMb) (for reference), murine neuroglobin (Ngb), and HGbI are shown in Fig. 1. Castp identified the distal pocket and the four xenon cavities [35] in SPMb (Fig. 1a). Ngb (Fig. 1b) has an extended distal pocket [36], into which two of its four experimentally-determined xenon binding pockets are incorporated [37]. The other two xenon atoms bind into surface pockets, and are not shown in Fig. 1b. Ngb does not have a proximal xenon binding site [37], and Castp does not identify one. HGbI has an extended distal pocket resembling that of Ngb (Fig. 1c). In addition, there is a tunnel in the surface which ends near the large internal cavity (lower right, Fig. 1c). The residues comprising the tunnel's surface opening are Leu(EF4)68, Leu(F1)75, Ile(H14)125, and Val(H18)129. The residues which separate the tunnel's interior end from the main cavity are Leu(E18)61 and Val(H11)122. Like Ngb, there appears to be no proximal binding pocket.

Exits from HGbI during our simulations are tabulated in Table 1. Of 50 five-nanosecond LES trajectories, O_2 remained inside HGbI in 21, and exited in 29. Ex1, Ex2 and Ex3, the exits through which more than one molecule passed, are shown in Figs. 2, 3, and 4. The most common

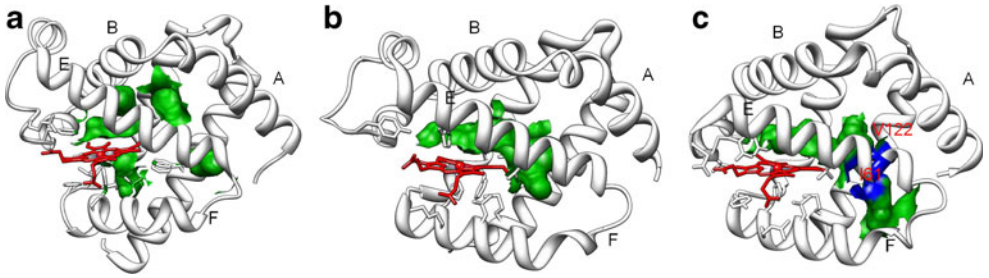

Fig. 1 Internal cavities from castp in **a**) myoglobin (PDB 1A6G), **b**) murine neuroglobin (PDB 1 W92) and **c**) HGbI (PDB 3S1I) plotted in green against the protein backbone as ribbons, and the heme in red tubes. Helices A, B, E, and F are labeled. In **c**), blue highlights residues which separate the main cavity from the tunnel. Portions of the surface bounded by these residues are also colored blue. Corresponding residues in red text for contrast. Because the Xe cavity volumes in SPMb were>40 Å^3, no cavities with smaller volumes are shown in **b**) and **c**)

exit, Ex1, was between residues Leu(EF4)68, Ile(F-2)72, Ile (H14)125, Val(H18)129. (Ile72 is numbered F-2 because the F helix begins four residues earlier in HGbI than SPMb. We adopted this scheme in order to preserve the usual numbering for most of the F helix). These exit residues are consistent with the tunnel identified by Castp in the crystal structure (Figs. 1c and 2). Anselmi et al. [28] calculated no homologous exits, but exit 5 of Bocahut et al. [29] is in the EF loop, hence similar to HGbI Ex1. A truncated hemoglobin from *Chlamydomonas eugametos* (Ce-trHb) also has an exit consisting of residues in the EF loop and H helix [38], as does *Drosophila melanogaster* hemoglobin (DmHb) [11].

The second most commonly observed exit, Ex2, was between the E and F helices in the vicinity of residue Thr(F0)74 (Fig. 3). The precise location varied, with exit occurring close to Gln(E13)56, Asp(F3)77, Leu(F4)78, or Arg(F7)81, or on the other side of Thr(F0)74, near Ile(E17)60 and Gly(EF6)70. It resembles portal 3 identified in SPMb by Ruscio et al. [20].

The third most common exit, Ex3, was between Asp (G10)97, Leu(G13)100, Thr(H9)120, and Y(H12)123 (Fig. 4). Exit 1 in Ngb [29] is between the G and H helices, at approximately the tenth position in both helices, similar to Ex3 in HGbI. Human cytoglobin also has exits between the G and H helices, designated P3, P3' and P3" [9], as does DmHb [11].

The most common CO exit in SPMb identified by Ruscio et al. [20] is via the distal (direct) pathway, with residues His (E7)64, Thr(E10)67 and the heme forming the exit. The second most common CO exit consists of Ala(E14)71, Ala (E17)74, Ile(E18)75, His(EF5)82, Glu(EF8)85, and Leu (F4)89. This is in roughly the area of Ex2 in HGbI. The third most traveled exit in SPMb consists of Lys(G2)101, Gln(G5)104, Arg(H16)139, Ala(H20)143, and Tyr (H23)146, that is, between the G and H helices, but closer to the C-terminal of the H helix than in HGbI or Ngb.

Exit Ex6 in HGbI, sampled only once, was on the other side of the G helix from Ex3, with Asp(G10)97 common to both exits, but with Glu(B17)36, Leu(G7)94, and Cys (G11)98 in Ex6. (Lack of a D helix creates a CE turn in HGbI). Exit E4 was between the distal side of the heme and residues Y(B10)29, F(B14)33, and F(C8)43. Exit Ex5, also sampled only once, was between Lys(G14)101, Gln

Table 1 Summary of O_2 exits from HGbI

Exit	Residues comprising exit	No. of occurrences
Ex1	Leu(EF4)68, Ile(F-2)72[a], Ile(H14)125, Val(H18)129	16
Ex2	Thr(F0)74[a]+Gln(E13)56, Asp(F3)77, Leu(F4)78, Arg(F7)81 or Thr(F0)74+Ile(E17)60, Gly(EF6)70	6
Ex3	Asp(G10)97, Leu(G13)100, Thr(H9)120, Y(H12)123	3
Ex4	Y(B10)29, F(B14)33, F(C8)43	1
Ex5	Lys(G2)101, Gln(G5)104, Lys(H5)116	1
Ex6	Glu(B17)36, Leu(G7)94, Asp(G10)97, Cys(G11)98	1

[a] The F helix begins four residues earlier in HGbI than in SPMb. We have designated these residues F-3, F-2, F-1, and F0 in order to retain homologous numbering in the remainder of the F helix

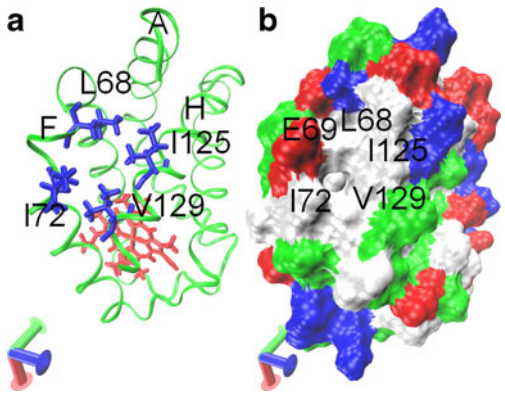

Fig. 2 **a** Ribbon rendering of HGbI from PDB 3S1I with the residues of Ex1 in blue tubes and the heme in red. Foreground helices A, F, and H are labeled, as are the exit residues. **b** Surface rendering of the same view as in **a**), colored by residue type (red = acidic, blue = basic, green = polar, white = apolar), with the exit residues labeled. E69 is not part of the exit, and is labeled because it appears close in this view. That Ex1 is within an irregular depression is only apparent when the protein surface is rendered

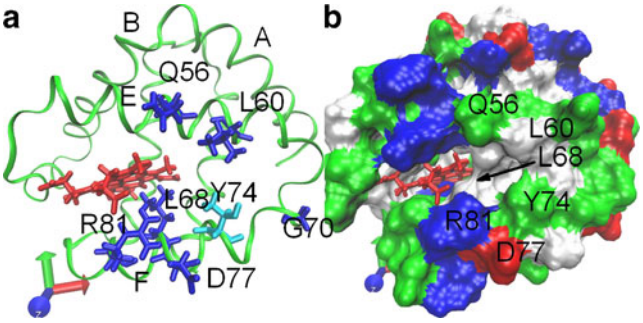

Fig. 3 **a** Ribbon rendering featuring HGbI exit Ex2 as in Fig. 2. Ex2 has closely spaced branches, separated by Y74, which is rendered light blue. Otherwise, the coloring is as in Fig. 2, with helices A, B, E, F labeled for reference. **b** Surface rendering by residue type of same view as in **a**). It is only apparent in this view that both branches are within surface depressions. L70 does not show in this view: during MD this region of HGbI rearranges to place L70 at the surface and in proximity to Y74. Note the low surface ridge between L60 and Y74 which appears to separate the branches of this exit

(G17)104, and Lys(H5)116 (yet another position between the G and H helices).

There were four incidences of O_2 traveling to the protein surface, re-entering and migrating through the protein again before finally diffusing into the solvent. In an additional trajectory, the oxygen re-entered twice. Three exits were not "clean": O_2 tumbled along the surface after exiting and before diffusing away from the protein. Similar behavior has been observed in LES calculations on Mt-trHbO [12]. In all of the trajectories in which O_2 did not exit HGbI within the 5 ns simulation time, there was an interval in which the O_2 diffused past the protein surface, but did not continue into the solvent. Rather, it reentered the protein and continued to migrate within the cavity until the simulation ended. One such case is illustrated in Fig. 5. Oxygen reentry has also been observed in LES studies of three different truncated hemoglobins [38]. The exits in human neuroglobin are in hydrophobic surface patches [39]. This is not the case for HGbI (Figs. 2, 3, and 4) or SPMb. The channels themselves are predominantly hydrophobic in HGbI, as in other globins.

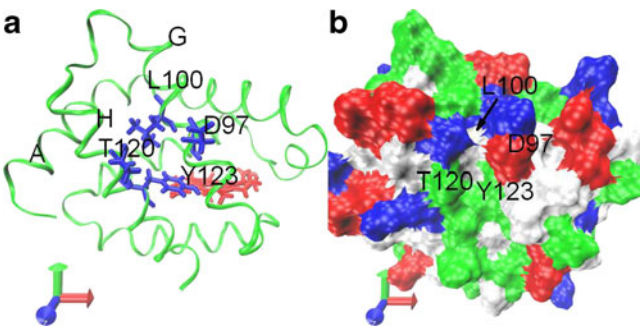

Fig. 4 **a** Ribbon rendering featuring HGbI exit Ex3 as in Fig. 2. Helices A, G, and H are labeled for reference. **b** Surface rendering by residue type of same view as in **a**). Ex3 is also within a surface depression

We analyzed the volume occupancy of O_2 in our trajectories (Fig. 6) in order to identify possible transient ligand docking sites in HGbI, and to compare their location with the Xe binding sites [37] in Ngb. HGbI has three transient ligand docking sites when the surface at 80 % of maximum occupancy is plotted. Two of these occur at homologous positions to two of the Xe sites in Ngb. When the 50 % surface is examined, two of these sites have coalesced, and the other is significantly extended.

In order to gauge the contribution of heme-protein interactions to protein rigidity around the heme, we calculated hydrogen-bond population frequencies. Since the heme propionates are ionized in physiological conditions, the interaction has an electrostatic component with angular criteria less stringent than true H-bonding. These calculations use H-bonding geometric criteria, and thus possibly underestimate the duration of interaction. The results are compiled in Table 2; HGbI has significantly more protein-heme propionate interactions than SPMb.

Discussion

The largest interior cavity in crystalline SPMb is a classical distal pocket concentrated in the volume above the heme. In HGbI, the distal pocket extends through the protein to the vicinity of residues Leu(F1)75 and Val(H11)122, similar to murine Ngb. HGbI differs from Ngb in having a tunnel in the crystal structure originating at Ex1, which is gated to the main internal cavity. A cavity spanning the vicinity of the heme to the opposite surface has also been observed in *Mycobacterium tuberculosis* truncated hemoglobin N (Mt-trHbN) [40].

A large internal cavity gated to the globin surface far from the heme results in a different balance in the possible exits between HGbI and Ngb. Ex1 (EF turn and H helix) was by far the most common exit from HGbI. In murine Ngb, on the other hand, the most common exit was between the AB turn and G helix [28]. The three most common exits found in our simulations have analogues in other globins, as discussed above. Ex1 and Ex3 have analogs in Ngb, cytoglobin and globins from invertebrates, while Ex2 is related to an exit in SPMb.

Ex1 is far from the heme end of HGbI. Simulations have identified other globlins with exits at the surface roughly opposite the heme. In addition to Ce-trHb [38] and DmHb [11], the *Cerebratulus lacteus* globin has exits designated T5 and T6 [10]. T5 consists of Ile(E19)56, Leu(H1)98, and Ala(H4)101, while T6 consists ofAla(F2)62, Ala(H4)101, and Asp(H7)104.

HGbI shares the characteristic that occasionally a ligand tumbles along the protein surface before diffusing away with Mt-trHbO [12]. Ligand reentry has been observed in

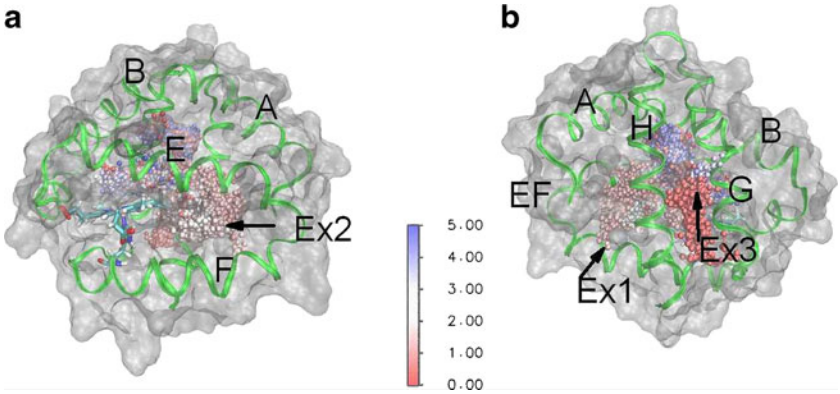

Fig. 5 A trajectory in which O_2 has not exited in 5 ns. The protein surface at 2.5 ns is plotted transparent gray. The protein backbone is rendered as green ribbons. Foreground helices & the EF turn (**b**) are labeled. O_2 is shown in "time lapse": its position in each frame is shown, and colored according to the color bar (labeled in ns). The heme is rendered in tubes colored by element (left side of a). Arrows mark the point of ligand exit via Ex2 (**a**), Ex1 and Ex3 (**b**). Note that O_2 visits Ex3 at two different times in the trajectory (*red and white*)

simulations of truncated hemoglobins [38], though not to the same extent as in HGbI.

We detected only two transient ligand docking regions in HGbI, which roughly coincide with two of the xenon binding sites observed experimentally in Ngb. These two xenon pockets are homologous to two of the xenon sites observed in SPMb [37]. Anselmi et al. [28]and Lutz et al. [30] observed transient ligand docking pockets in Ngb corresponding to all the xenon binding sites in SPMb.

The absence of a D helix reduces the volume available directly above the heme (Fig. 1). However, the presence of a large interior cavity offset from the heme in Ngb suggests that steric hindrance in the distal region is not the only factor influencing development of such a cavity. A large interior cavity implies that ligands may more easily traverse the interior of HGbI or Ngb than SPMb, with comparatively less ligand exit from the vicinity of the heme (direct pathway). Anselmi et al. [28] observed no exits via the direct pathway in Ngb, and Bocahut et al. few such exits [29].

Further inflexibility in the distal region of HGbI is provided by interactions between protein and the heme propionate groups (Table 2); there are three interactions in HGbI which are at least as persistent as the one protein/propionate interaction in SPMb. The internal volume accessible to ligand in HgbI (Figs. 1, 5 and 6), has a gate consisting of L61, I65, and V122, and another nearby consisting of L61

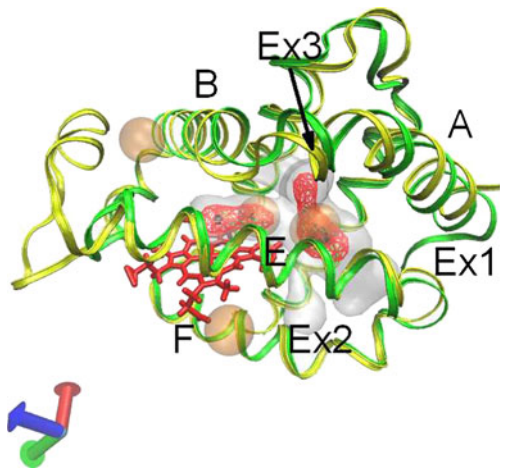

Fig. 6 Ligand occupancies in HGbI (*green ribbon*) with heme as red tubes, and helices *A*, *B*, *E* and *F* labeled. Ngb (PDB 3GLN) (*yellow ribbon*) has been aligned to HGbI. The orange spheres are the Xe in PDB 3GLN. The three black surfaces are the occupancy contours for 80 % of maximum O_2 occupancy in HGbI. The largest and rightmost is partially obscured by Xe from Ngb. Red wireframe is the occupancy contour for 50 % of maximum (two surfaces). The transparent gray surface is the 10 % of maximum occupancy contour. It extends to Ex1, Ex2, and Ex3 (out the back of this view)

Table 2 Protein-heme interactions and their persistence

Donor heavy atom	Acceptor (propionate O)	HGbI frequency (%)	SPMb frequency (%)
Gln44 bbN[a]	O1D[b]	20 (10)[c]	
Gln44 bbN	O2D	**80 (10)**	
Asn45 bbN	O1D	20 (10)	
Asn45 bbN	O2D	60 (30)	
Asn45 ND2	O1D	20 (10)	**70 (20)**[d]
Asn45 ND2	O2D	50 (6)	
Arg81 side NH	O1A	40 (10)	
Arg81 side NH	O2A	60 (6)	
Arg81 side NE	O1A	50 (1)	
Arg81 side NE	O2A	**70 (6)**	
Tyr85 OH	O1A	20 (10)	
Tyr85 OH	O2A	**70 (10)**	

[a] *bb* backbone

[b] Other atom names are standard PDB atom names

[c] averaged over three 5-ns trajectories. Standard deviations are in parentheses; H-bonds persisting≥70 % are in bold face

[d] homologous position in SPMb is Arg45

and the heme edge. These gates are more open in HgbI than SPMb, as is evident from Figs. 5 and 6. Figures 2, 3, 4, and 5 suggest that the tendency for O_2 to remain near exits may be due to surface depressions, present even in the static crystal structure. These depressions may provide transient docking sites for O_2, though residence times were so short they did not show up in the ligand occupancy contours (Fig. 6).

Conclusions

HGbI is most homologous to Ngb among the globins whose crystal structures have been obtained. Both globins have extended internal cavities offset from the heme, although Ngb has a D helix, and presumably more flexible distal region. Our calculations show that HGbI has two transient ligand docking pockets. They overlap homologous Xe pockets (and ligand docking sites) in Ngb. We did not detect additional ligand binding sites, as simulations on Ngb have done. We see exit from three portals sampled more than once during our studies, and three more sampled only once. The three multiply-sampled exits have homologs in other previously-studied globins. We are unaware of a globin with homologs of all three of the HGbI exits. Six exits are a typical number for the globins studied to date. More unusually, in HGbI ligand may tumble along the protein surface before diffusing away from it, and ligand reentry from the protein surface is a common event.

Our simulations indicate that the HGbI surface contains depressions at the three most-sampled ligand exits, in which ligand may reside briefly. This property may contribute both to rapid oxygen uptake of the protein, and the slow off-rate, enhancing the tendency toward these characteristics provided by the Tyr/Gln distal residues. Ligand uptake in globins requires collisions between bodies of significantly different size. Only collisions at a small percentage of the protein surface area (at the portals) can result in ligand uptake. The portal must also be in a conformation which permits ligand entry as the collision occurs. If a ligand stays near the portal, its chances of being close enough to the protein during a suitable protein conformation may be increased. In the exit process, increasing the oxygen residence time near the gate increases the probability of reentry, resulting in net slower de-oxygenation than in globins without such depressions. The magnitude of the effect can be gauged from the following: in each of the trajectories in which ligand did not exit the protein, O_2 visited an exit, but reentered. Had each ligand entered solvent at its first surface visit, as has been observed in most of the ligand migration studies, all 50 of the oxygen molecules whose trajectories were calculated in this study would have exited within 5 ns, instead of 29. The high incidence of reentry in HGbI seems unique among the systems studied to date.

Acknowledgments This work was supported by the U.S. Army Telemedicine and Advanced Technology Research Center (W81XWH0520013) to M.A. We wish to thank the Extreme Science and Engineering Discovery Environment (then TeraGrid) for a generous grant of supercomputing time (TG-MCB090178). We are also very grateful to the reviewers for their insightful comments.

References

1. Vinogradov SN, Moens L (2008) Diversity of globin function: enzymatic, transport, storage, and sensing. J Biol Chem 283 (14):8773–8777
2. Dunfield PF, Yuryev A, Senin P, Smirnova AV, Stott MB, Hou S, Ly B, Saw JH, Zhou Z, Ren Y et al. (2007) Methane oxidation by an extremely acidophilic bacterium of the phylum Verrucomicrobia. Nature 450:879–882
3. Teh A-H, Saito JA, Baharuddin A, Tuckerman JR, Newhouse JS, Kanbe M, Newhouse EI, Rahim RA, Favier F, Didierjean C et al. (2011) Hell's Gate globin I: an acid and thermostable bacterial hemoglobin resembling mammalian neuroglobin. FEBS Lett 585:3250–3258
4. de Baere I, Perutz MF, Kiger L, Marden MC, Poyart C (1994) Formation of two hydrogen bonds from the globin to the heme-linked oxygen molecule in *Ascaris* hemoglobin. Proc Natl Acad Sci USA 91 (1594–1597)
5. Wajcman H, Kiger L, Marden MC (2009) Structure and function evolution in the superfamily of globins. C R Biologies 332(2–3):273–282
6. Elber R, Karplus M (1990) Enhanced sampling in molecular dynamics: use of the time-dependent Hartree approximation for a simulation of carbon monoxide diffusion through myoglobin. J Am Chem Soc 112:9161–9175
7. Ulitsky A, Elber R (1994) Application of the Locally Enhanced Sampling (LES) and a Mean Field with a Binary Collision Correction (cLES) to the Simulation of Ar Diffusion and NO Recombination in Myoglobin. J Phys Chem 98(1034–1043)
8. Czerminski R, Elber R (1991) Computational studies of ligand diffusion in globins: I. Leghemoglobin. Proteins: structure, function, and. Genetics 10(1):70–80
9. Orlowski S, Nowak W (2007) Locally enhanced sampling molecular dynamics study of the dioxygen transport in human cytoglobin. J Mol Model 13:715–723
10. Orlowski S, Nowak W (2007) Oxygen diffusion in minihemoglobin from *Cerebratulus lacteus*: a locally enhanced sampling study. Theor Chem Acc 11:253–258
11. Dams L, Orlowski S, Nowak W (2008) Computer modeling of small ligands diffusion in Drosophila Melanogaster hemoglobin. Proc Comput Biophys Syst Biol (CBSB08) 40:714–717
12. Heroux MS, Mohan AD, Olsen KW (2011) Ligand migration in the truncated hemoglobin of *Mycobacterium tuberculosis*. IUBMB Life 63:214–230
13. Shadrina M, English AM, Peslherbe GH (2012) Effective simulations of Gas diffusion through kinetically accessible tunnels in multisubunit proteins: O2 pathways and escape routes in T-state deoxyhemoglobin. J Am Chem Soc 134:11177–11184
14. Nutt DR, Meuwly M (2004) CO migration in native and mutant myoglobin: atomistic simulations for the understanding of protein function. Proc Natl Acad Sci USA 101(16):5998–6002
15. Hummer G, Schotte F, Anfinrud PA (2004) Unveiling functional protein motions with picosecond x-ray crystallography and molecular dynamics simulations. Proc Natl Acad Sci USA 101(43):15330–15334

16. D'Abramo M, Nola AD, Amadei A (2009) Kinetics of carbon monoxide migration and binding in solvated myoglobin as revealed by molecular dynamics simulations and quantum mechanical calculations. J Phys Chem B 113:16346–16353
17. Anselmi M, Aschi M, Nola AD, Amadeiz A (2007) Theoretical characterization of carbon monoxide vibrational spectrum in sperm whale myoglobin distal pocket. Biophys J 92:3422–3447
18. Bossa C, Anselmi M, Roccatano D, Amadei A, Vallone B, Brunori M, Nola AD (2004) Extended molecular dynamics simulation of the carbon monoxide migration in sperm whale myoglobin. Biophys J 86:3855–3862
19. Tsuduki T, Tomita A, S-y K, S-i A, Yamato T (2012) Ligand migration in myoglobin: a combined study of computer simulation and x-ray crystallography. J Chem Phys 136(165101)
20. Ruscio JZ, Kumar D, Shukla M, Prisant MG, Murali TM, Onufriev AV (2008) Atomic level computational identification of ligand migration pathways between solvent and binding site in myoglobin. Proc Natl Acad Sci USA 105:9204–9209
21. Huang X, Boxer SG (1994) Discovery of new ligand binding pathways in myoglobin by random mutagenesis. Nat Struct Biol 1:226–229
22. Schotte F, Lim M, Jackson TA, Smimov AV, Soman J, Olson JS, Phillips GNJ, Wulff M, Anfinrud PA (2003) Watching a protein as it functions with 150-ps time-resolved x-ray crystallography. Science 300:1944–1947
23. Srajer V, Ren Z, Teng T-Y, Schmidt M, Ursby T, Bourgeois D, Pradervand C, Schildkamp W, Wulff M, Moffat K (2001) Protein conformational relaxation and ligand migration in myoglobin: a nanosecond to millisecond molecular movie from time-resolved Laue X-ray diffraction. Biochemistry 40:13802–13815
24. Elber R (2010) Ligand diffusion in globins: simulations versus experiment. Curr Opin Struct Biol 20(2):162–167
25. Maragliano L, Cottone G, Ciccotti C, Vanden-Eijnden E (2010) Mapping the network of pathways of CO diffusion in myoglobin. J Am Chem Soc 132:1010–1017
26. Cohen J, Arkhipov A, Braun R, Schulten K (2006) Imaging the migration pathway for O2 Co, NO, and Xe inside myoglobin. Biophys J 91(9):1844–1857
27. Cohen J, Olsen KW, Schulten K (2008) Finding gas migration pathways in proteins using implicit ligand sampling. Methods Enzymol 437:439–455
28. Anselmi M, Nola AD, Amadei A (2011) Kinetics of carbon monoxide migration and binding in solvated neuroglobin as revealed by molecular dynamics simulations and quantum mechanical calculations. J Phys Chem B 115:2346–2446
29. Bocahut A, Bernad S, Sebban P, Sacquin-Mora S (2009) Relating the diffusion of small ligands in human neuroglobin to its structural and mechanical properties. J Phys Chem B 113:16257–16267
30. Lutz S, Nienhaus K, Nienhaus GU, Meuwly M (2009) Ligand migration between internal docking sites in photodissociated carbonmonoxyneuroglobin. J Phys Chem B 113:15334–15343
31. Phillips JC, Braun R, Wang W, Gumbart J, Tajkhorshid E, Villa E, Chipot C, Skeel RD, Kale L, Schulten K (2005) Scalable molecular dynamics with NAMD. J Comput Chem 26:1781–1802
32. Humphrey W, Dalke A, Schulten K (1996) VMD - Visual Molecular Dynamics. J Molec Graphics 14:33–38
33. Dundas J, Ouyang Z, Tseng J, Binkowski A, Turpaz Y, Liang J (2006) CASTp: computed atlas of surface topography of proteins with structural and topographical mapping of functionally annotated residues. Nucleic Acid Res 34:W116–W118
34. Pettersen E, Goddard T, Huang C, Couch G, Greenblatt D, Meng E, Ferrin T (2004) UCSF Chimera–a visualization system for exploratory research and analysis. J Comput Chem 25:1605–1612
35. Tilton RF, Kuntz ID, Petsko GA (1984) Cavities in proteins: structure of a metmyoglobin-xenon complex solved to 1.9 Å. Biochemistry 23:2849–2857
36. Pesce A, Dewilde S, Nardini M, Moens L, Ascenzi P, Hankeln T, Burmester T, Bolognesi M (2003) Human brain neuroglobin structure reveals a distinct mode of controlling oxygen affinity. Structure 11:10878–11095
37. Moschetti T, Mueller U, Schulze J, Brunori M, Vallone B (2009) The structure of neuroglobin at high Xe and Kr pressure reveals partial conservation of globin internal cavities. Biophys J 97:1700–1708
38. Golden SD, Olsen KW (2008) Identification of ligand-binding pathways in truncated hemoglobins using locally enhance sampling molecular dynamics. Methods Enzymol 437:457–473
39. Orlowski S, Nowak W (2008) Topology and thermodynamics of gaseous ligands diffusion paths in human neuroglobin. Biosystems 94(263–266)
40. Bidon-Chanal A, Martı' MA, Crespo A, Milani M, Orozco M, Bolognesi M, Luque FJ, Estrin DA (2006) Ligand-induced dynamical regulation of NO conversion in mycobacterium tuberculosis truncated hemoglobin-N. Proteins 64:457–464